17th World Conference on Earthquake Engineering, 17WCEE
Sendai, Japan - September 13th to 18th 2020

VALUE CASE FOR THE USE OF SEISMICALLY ISOLATED LIGHT-FRAME WOOD BUILDINGS IN NEW ZEALAND

T.C. Francis [1], T.J. Sullivan [2], A. Filiatrault [3], [4]

[1] *PhD Student, Department of Civil and Natural Resources Engineering, University of Canterbury, tom.francis@pg.canterbury.ac.nz*
[2] *Professor, Department of Civil and Natural Resources Engineering, University of Canterbury, timothy.sullivan@canterbury.ac.nz*
[3] *Professor, Department of Civil, Structural and Environmental Engineering, State University of New York at Buffalo, af36@buffalo.edu*
[4] *Professor, University School for Advanced Studies IUSS Pavia, andre.filiatrault@iusspavia.it*

Abstract

New Zealand residential buildings are typically made of light-frame wood construction with gypsum wallboards contributing to the structural strength and stiffness. Such buildings typically perform well in earthquakes with minimal casualties, as was demonstrated in Christchurch during the 2011 Canterbury earthquake sequence. However, damage was widespread and even minor cracking of gypsum wallboards required invasive repairs, which displaced large numbers of the population and cost $16 billion NZ dollars, as well as contributing negatively to the livelihood of those affected. High damage costs were similarly reported in the 1994 Northridge earthquake in California and the1995 Kobe earthquake in Japan. These high damage costs have prompted researchers to investigate methods for reducing seismic loss to these residential buildings through the development of low damage design systems, such as seismic isolation. Seismic isolation has been used very successfully to protect larger commercial and industrial buildings from earthquakes around the world. Research in Japan in the early 2000s and later in the United States and New Zealand showed that seismic isolation could also be used effectively on light-frame wood buildings with sliding type devices such as friction pendulums.

This paper presents a value case for the use of seismic isolation in New Zealand residential buildings by comparing the expected annual loss for fixed-base and seismically isolated light-frame wood buildings. First, a wind load analysis is undertaken to determine the combination of seismic weight and isolation friction coefficient required to provide adequate seismic protection, while minimizing the risk of buildings moving under strong wind gusts. A vulnerability analysis is then undertaken to determine appropriate vulnerability functions for seismically isolated light-frame wood buildings. In the methodology presented in this paper, loss data generated by insurance claims information from the 2011 Christchurch Earthquake is used to determine vulnerability functions for the current housing stock. By further considering the loss attributed to drift and acceleration sensitive non-structural components and using a simplified single degree of freedom building model subjected to nonlinear analyses, vulnerability functions for seismically isolated buildings are developed. The vulnerability is shown to reduce significantly for isolated buildings compared to that of equivalent fixed-base buildings. The fixed-base and seismically isolated vulnerability functions are then used to compare expected annual losses. Results indicate that losses are significantly reduced for the seismically isolated building models. As such, if low-cost isolation systems can be developed there would appear to be a strong value case for such systems.

Keywords: Seismic Isolation; Light-frame wood; Expected annual loss; Residential buildings.

1 Introduction

The 2011 Canterbury earthquake sequence caused extensive damage to residential buildings. While a large amount of damage, particularly in Christchurch's eastern suburbs, was due to soil effects such as liquefaction, it is evident that a significant portion of the damage could be attributed to excessive drift and acceleration demands in the superstructure [1]. Storey drift in particular has been shown to be a key parameter for the control of damage experienced by light-frame wood framed buildings [2], and therefore it is desirable to implement seismic systems that limit drift demands. New Zealand residential buildings are typically made of light-frame wood construction, with gypsum wallboards constituting the primary structural system to provide lateral strength and stiffness. From a life-safety perspective, well-designed light-frame wood buildings typically perform well in earthquakes, as evidenced by the limited loss of life in the 1994 Northridge Earthquake (6.7 M_w) in the United States (US), the 1995 Kobe Earthquake (6.9 M_w) in Japan and the 2011 Christchurch Earthquake (6.2 M_w). However, these earthquakes still caused extensive and costly damage. Estimates after the Christchurch Earthquake sequence in 2010-2011 indicated losses to residential buildings to be approximately NZ$16 billion of the $40 billion total building and infrastructure losses [3, 4]. This $40 billion loss accounted for approximately 20% of New Zealand's GDP. These high damage costs have prompted researchers to investigate methods for reducing seismic loss to these residential buildings including the development of low damage design systems, such as seismic isolation.

Japan appears to be the first country to have investigated the use of seismic isolation for light-framed wood buildings after the 1995 Kobe earthquake, with the intent of researching methods that dealt with the flexibility issues of the commonly used rubber bearings of the time [5]. The first tests of seismically isolated wood-frame buildings with sliding isolators, which were identified as being the most promising technology, were also completed in Japan [6, 7]. In New Zealand applications of seismic isolation of light-frame wood residential houses is not reported in the literature. However, research into low cost isolation devices was undertaken by BRANZ, which indicated that high wind loads would be likely to activate traditional isolation systems under light-weight buildings [8]. In the US, seismically isolated light-frame buildings have been tested and at least one seismically isolated wood building has been constructed [9]. In addition, strengthening of the building through uni-body construction was also investigated to increase the strength of the walls and allow cheaper, high friction sliding devices to become practicable [10-12]. The uni-body construction requires all gypsum wallboards and stucco finishes participating in the resistance of lateral loads. However, in New Zealand, with different construction techniques that typically do not incorporate the use of stucco finishing, this method may not be practicable.

This paper proposes a method for determining the vulnerability of seismically isolated light-frame wood buildings, which are susceptible to high wind gusts. A value case for the use of seismic isolation is thereby provided through comparison of the expected annual loss (EAL) for fixed-base and seismically isolated light-frame wood buildings. Sensitivity analyses are conducted to validate the research.

2 Seismically Isolated Light-Weight Buildings Under High Wind Loads

It is desirable for the maximum expected wind loading on the structure to be less than the activation or yield loads of the seismic isolation devices. This will prevent the building from moving in strong wind gusts, which would unsettle the building occupants and could cause unwanted damage. In order to resist wind loads, it has previously been proposed [8] that the weight of the isolated building, $W_{isolated}$, be high enough in relation to the applied wind load, F_{wind}, through practical levels of friction coefficients. Assuming Coulomb friction, the relationship between the seismic isolation friction coefficient, μ, (alternatively the yield coefficient in the case of metallic type devices) and the ratio of the wind load and building weight can be simply expressed as:

$$\mu = \frac{F_{wind}}{W_{isolated}} \quad (1)$$

A wind loading analysis was completed by Thurston [8] to determine the required isolation coefficients for different concrete foundation thicknesses to prevent motion under strong wind gusts. The results are reproduced in this paper and extended to include thicker concrete foundations, up to 250 mm thick. A typical modern house layout has been considered for analysis. The house is a single storey dwelling, wood-framed with three bedrooms and a floor plan of 143 m^2 representing a small to medium size dwelling, which is close to the average house size of 149 m^2 for New Zealand in 2019. Different combinations of wall cladding and roof weights were considered giving 18 total configurations. The dead loads used for the seismic mass calculation are taken from [13] and shown in Table 1. Maximum expected wind loading was assessed using NZS 3604 [14] and corresponds to a return period of 2% in 50 years.

Table 1 – Dead loads for seismic mass calculations of the model buildings.

Application		Dead Load (kPa)
Roof	Light	0.20
	Heavy	0.60
Ceiling		0.24
Walls	Light	0.30
	Medium	0.80
	Heavy	0.22
Partitions (based on floor area)		0.20
Floor		0.60

The friction coefficient required to prevent sliding of the isolators was then calculated using Eq. (1). The friction coefficients required for high wind zones considering the 18 configurations of the house are shown in Fig. 1. New Zealand also has ‘very high’ and ‘extreme’ wind loading zones for certain locations, both corresponding to the same return period of 2% in 50 years although the number of houses built in these zones is small. Most houses in cities will be considered high wind zone or lower due to the presence of neighbouring buildings reducing wind-loading demands.

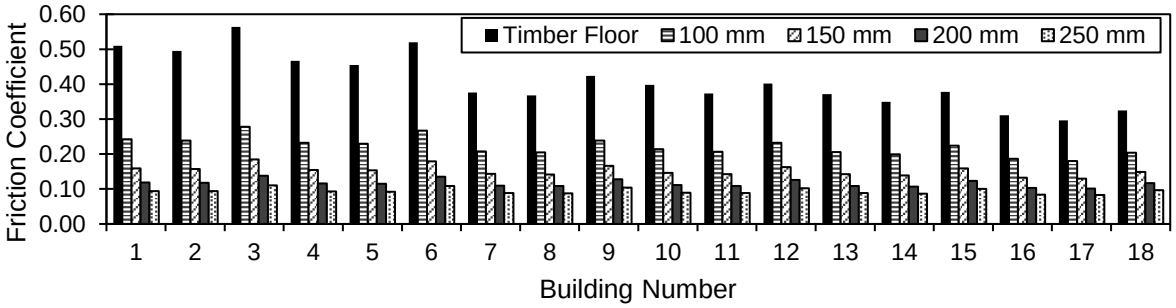

Fig. 1 – Required seismic isolator friction coefficient for 18 different building configurations with differing weights considering various cladding types, roof types, roof pitches and flooring system, for high wind zones.

The results in Fig. 1 show that relatively low coefficients of friction can be used for isolating light-frame wood buildings built on concrete flooring systems in a high wind zone regardless of cladding type if the concrete is thick enough. A friction coefficient of 0.1 could be considered appropriate for most building configurations in a high wind zone under a 250 mm thick slab. The effects

on floor plan area and number of storeys on the required coefficient of friction were also investigated but results were similar. The wellington region, one of New Zealand's highest seismic and wind loading areas, mainly falls into the 'high' wind zone category. An isolation coefficient of friction of 0.1 has therefore been used herein in the isolated building model for the vulnerability analysis.

3 Determination of Seismically Isolated Building Vulnerability Functions

In the absence of loss data for seismically isolated residential buildings, an approach for determining vulnerability functions of the isolated light-frame wood buildings is presented in this section. Firstly, the vulnerability function for fixed-base light-frame wood buildings is determined from loss data generated by insurance claim information after the 2010-2011 Canterbury earthquake sequence as shown in Fig. 2 [4]. Nonlinear time-history (NLTH) dynamic analyses are then used to assess the drift and acceleration response of a simple single degree of freedom (SDOF) fixed-base model calibrated to the typical strength and stiffness of New Zealand residential buildings. The NLTH dynamic analysis results are matched to the known vulnerability function to determine storey loss functions in terms of the engineering demand parameters (EDPs), drift, and roof acceleration. An identical but seismically isolated model is proposed which includes additional weight added to the superstructure through the thickening of the concrete foundation to reduce the ability of high wind loads to activate the isolation system. The isolated model is then analysed and used to determine vulnerability functions for seismically isolated buildings by using the storey loss functions previously generated.

3.1 Step 1: Review of known vulnerability of fixed-base light frame wood buildings

Horspool *et al.* [2] investigated the vulnerability of light-frame wood buildings that make up 95% of the residential building stock. The results of the Canterbury earthquake sequence and the extensive coverage of insurance through the Earthquake Commission (EQC) in New Zealand meant that there was a relatively comprehensive pool of insurance data made available for properties that lodged claims. This meant that effectively all residential buildings that had damage to a value of less than NZ$100,000 (the maximum building cover under EQC which, when exceeded, is covered by private insurance) had a repair cost estimate as well as a claim settlement amount recorded in the database. Coupled with the use of the ShakeMap software [15] for determining site ground motion intensities, this data allowed for possibly unprecedented access to loss information to aid accurate determination of vulnerability functions for light-frame wood buildings.

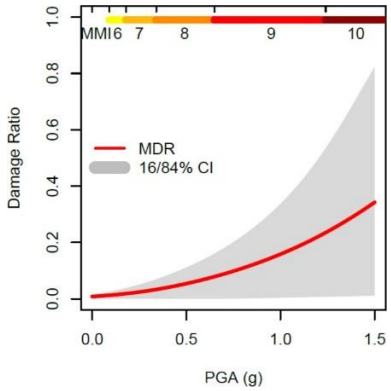

Fig. 2 – Structural loss versus PGA and MMI for light-framed wood houses from the Christchurch Earthquake Sequence [4].

The initial work by Horspool *et al.* [4] presented vulnerability functions in terms of Modified Mercali Intensity (MMI), but work has since expanded this to include the intensity measure of peak ground acceleration (PGA) as shown in Fig. 2. This represents loss as a damage ratio, which is defined

as the ratio of the repair cost over the replacement cost for the residential building typologies considered. It does not include loss to acceleration sensitive building components (e.g. house fittings such as white ware, electronics, heat pumps and services).

3.2 Step 2: Develop light-frame wood building model

The following is an outline of the approach taken and assumptions made to determine the model parameters of a seismically isolated SDOF light-frame wood structure that is representative of a standard New Zealand residential building. This model was developed using the RUAUMOKO software [16]. The model incorporates a Wayne-Stewart spring in RUAUMOKO (Fig. 3(a)) to model the earthquake resisting system of the house. The Wayne-Stewart model represents shear force and deformation of the gypsum panels typically found in New Zealand residential building and captures the pinching behaviour caused by screw-slip, the assumed deformation mechanism for typical New Zealand gypsum walls. The model was calibrated to the results of cyclic testing of a New Zealand house conducted by Thurston [17] prior to the 2011 Christchurch Earthquake and so was not earthquake damaged. The test house had a light-weight roof and light-weight weatherboard cladding. The floor plan is shown in Fig. 3(c). The original building was on a timber foundation, as opposed to a rigid concrete foundation considered in the model. However, it was assumed the foundation type did not significantly affect the results of the racking test. The period of vibration of the test building was found to be 0.05 s from snap-back testing. This relatively short period reflects the stiff nature of the un-cracked gypsum wall panels compared to light-frame wood buildings with plywood panels as the seismic force-resisting system.

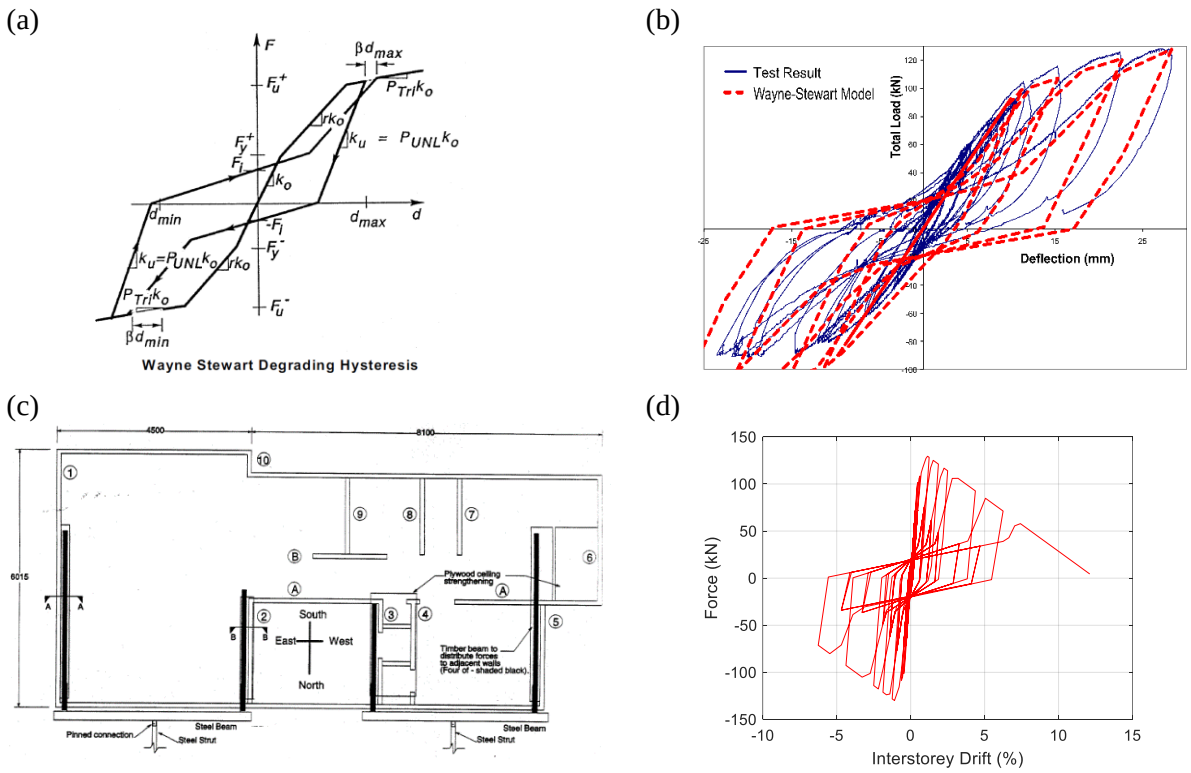

Fig. 3 – (a) Visual representation of the Wayne-Stewart hysteresis loop and its parameters from the RUAUMOKO Appendices [18], (b) a comparison of the Wayne-Stewart degrading hysteresis model to the cyclic testing results of a typical New Zealand light-frame wood house, (c) the floor plan of the cyclic test building, and (d) the CUREe cyclic analysis results for the Wayne-Stewart model.

The values and a description of the parameters used for the Wayne-Stewart hysteresis spring model in Fig. 3(b) are provided in Table 2. The parameters were selected to match the initial elastic and

post-yield behaviour of the test building. The test building was only displaced by 25 mm corresponding to a drift of 1.04%. At this drift, the building was assumed to have reached its ultimate strength capacity as the wall on grid line 1 had failed [17]. Beyond this drift level, the strength decreased with increasing displacement, as shown in Fig. 3(d). The hysteresis in Fig. 3(d) was subjected to the standard CUREe cyclic loading protocol to show the post ultimate behaviour of the house.

Table 2 – Parameters for the Wayne-Stewart hysteresis spring (Fig. 3(a)).

Symbol	Property Description	Parameter Value
FU	Ultimate force or moment	130 kN
FY	Yield force or moment	100 kN
FI	Intercept force or moment	20 kN
PTRI	Tri-linear factor beyond ultimate force or moment	-0.05
PUNL	Unloading stiffness factor	1.45
GAP+	Initial slackness, positive axis	0
GAP-	Initial slackness, negative axis	0
BETA	Beta or softening factor	1.09
ALPHA	Reloading or pinch power factor	0.45
LOOP		0

The fixed-base house model with the Wayne-Stewart hysteresis spring is illustrated in Fig. 4(a). The roof node has the in-plane translational degree-of-freedom released, while the in-plane rotational degree-of-freedom is fixed to allow shear deformation in the Wayne-Stewart spring. A bi-linear SPRING element in RUAUMOKO with a high initial stiffness and yield coefficient of 0.1 was then used to model the friction seismic isolation system. The base node of the house model was then released in the horizontal direction. Rotational restraint was still applied to model an isolator which only deforms in shear, typical of lead rubber bearings and friction type devices. The overall model can then be represented as a SDOF system with the base attached to the horizontal spring element, as in Fig. 4(b).

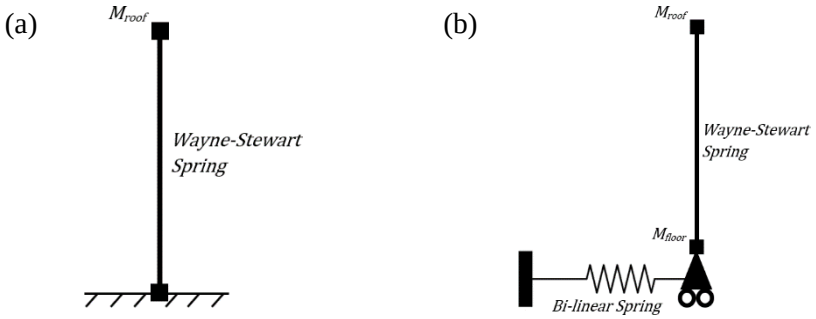

Fig. 4 – Comparison of the RUAUMOKO models for (a) a fixed-base light-frame wood house and (b) the same house with a bi-linear seismic isolation system added.

The mass of the building was lumped at the roof and isolation levels. For this simple model, the seismic weight was calculated using Table 2. The roof weight was found to be 50 kN, which was based on a single storey house with a floor area of 75 m^2. In the fixed-base building model this roof mass is all that is required. However, removal of the base fixity and addition of a horizontal spring to model the isolation components incorporates another degree of freedom to the model, which will likely have a significant seismic mass contribution. This mass can be associated with the weight of the flooring system and any building contents. Again using Table 2, the weight of the floor and isolation system was found to be 481 kN, assuming that a 250 mm thick concrete floor was required for sufficient mass to

overcome wind loading in a high-wind zone. This corresponds to a required isolation friction coefficient of approximately 0.1 for high wind zones, as shown in Fig. 1.

As P-Delta effects can be potentially significant in the prediction of the response of light-frame wood buildings, large displacement analyses were included. The seismic weight was applied in the horizontal direction only. The NLTH dynamic analyses were conducted using the Newmark constant (average) acceleration integration method with an integration time-step of 0.005 seconds. The damping matrix was based on the Wilson-Penzein damping model with a linear variation of damping with elastic natural frequencies. One percent damping was specified on the first mode which is in line with other models for light-frame wood buildings where the hysteretic model accounts for most of the damping and only a small amount of additional viscous damping is required [19, 20].

3.3 Step 3: Ground motions selection

Ground motions for the NLTH dynamic analyses were taken from the work by Yeow *et al.* [21], which used the results of probabilistic seismic hazard analysis (PSHA) together with the generalised conditional intensity measure (GCIM) method [22] to determine scaling factors for a selection of earthquake records. PSHA was performed for Wellington for V_{s30} = 450 ms^{-1} on OpenSHA using New Zealand-specific rupture forecast models and attenuation relationships for spectral acceleration at 0.5 seconds, S_a(0.5 s). Refer to [21] for further details of the ground motions and the scaling process. The conditioning period of 0.5 seconds was selected because it is relatively close to the elastic first mode period of the building model of T_1 = 0.15 seconds. Nine hazard levels of 20 orthogonal (horizontal) records were considered the corresponding hazard level, probability of occurrence in 50 years (P_{50}), and annual rate of exceedance (v), outlined in Table 3.

The vulnerability function for fixed-base houses is in terms of PGA. However, the ground motions used for the NLTH dynamic analyses are conditioned on S_a(0.5 s). To relate the intensity of the ground motions for Sa(0.5 s) to PGA, Eq. (2) from Bradley *et al.* [23] was used. This determines PGA based on the annual rate of exceedance, v,

$$\mathrm{PGA} = \mathrm{PGA}_{\mathrm{asy}} \exp\left[\alpha \left\{ \ln\left(\frac{\mathrm{v}}{\mathrm{v}_{\mathrm{asy}}}\right)\right\}^{-1}\right] \tag{2}$$

where PGA_{asy} is the vertical asymptote of the intensity measure, v_{asy} is the horizontal asymptote of the annual rate of exceedance, and α is a constant for fitting the hyperbolic model to PSHA data. For a Wellington site IM_{asy}, v_{asy}, and α take on values of 81.7 g, 6617 /year, and 75.9 respectively. Note

Table 3 – Comparison of S_a(0.5 s) and PGA intensities for a Wellington site at each of nine hazard levels with the corresponding rate of exceedance in 50 years, P_{50}, and annual rate of exceedance, v.

Hazard Level	P_{50} [%]	v	S_a(0.5 s) [g]	PGA [g]
1	80	0.0322	0.135	0.165
2	50	0.0139	0.248	0.246
3	20	0.00446	0.564	0.391
4	10	0.00211	0.991	0.511
5	5	0.00103	1.519	0.646
6	2	0.000404	2.275	0.847
7	1	0.000201	2.888	1.018
8	0.5	0.000100	3.546	1.207
9	0.2	0.000040	4.484	1.480

that Eq. (2) considers median values of the intensity measure. This procedure allows NLTH dynamic analysis results using the S_a(0.5 s) conditioned ground motions to be compared directly to the PGA

intensity measure of the fixed-base vulnerability function for residential buildings. The resulting PGA demands at each hazard level are shown in Table 3.

3.4 Step 4: Conduct nonlinear time-history dynamic analyses and determine median storey loss functions

Losses to residential buildings can be categorised as either acceleration-based or displacement-based. Acceleration effects typically cause damage to non-structural components and house contents while displacement demands can damage structural components such as gypsum wallboards. Analysis of data provided from EQC claim records indicated that one third of damage was attributed to contents loss which is assumed here as being acceleration sensitive. The remaining two thirds can be classified as drift sensitive loss. For simplicity, and due to high uncertainty in the loss attributed to acceleration sensitive contents, this analysis assumes the shaking intensity does not affect the ratio of acceleration to displacement-based loss.

NLTH dynamic analyses of both the fixed-base and isolated building models were conducted using the suite of ground motions, described in Section 3.3. The peak interstorey drift demand and peak roof acceleration are recorded for each ground motion as a function of the PGA. The results are shown in Fig. 5.

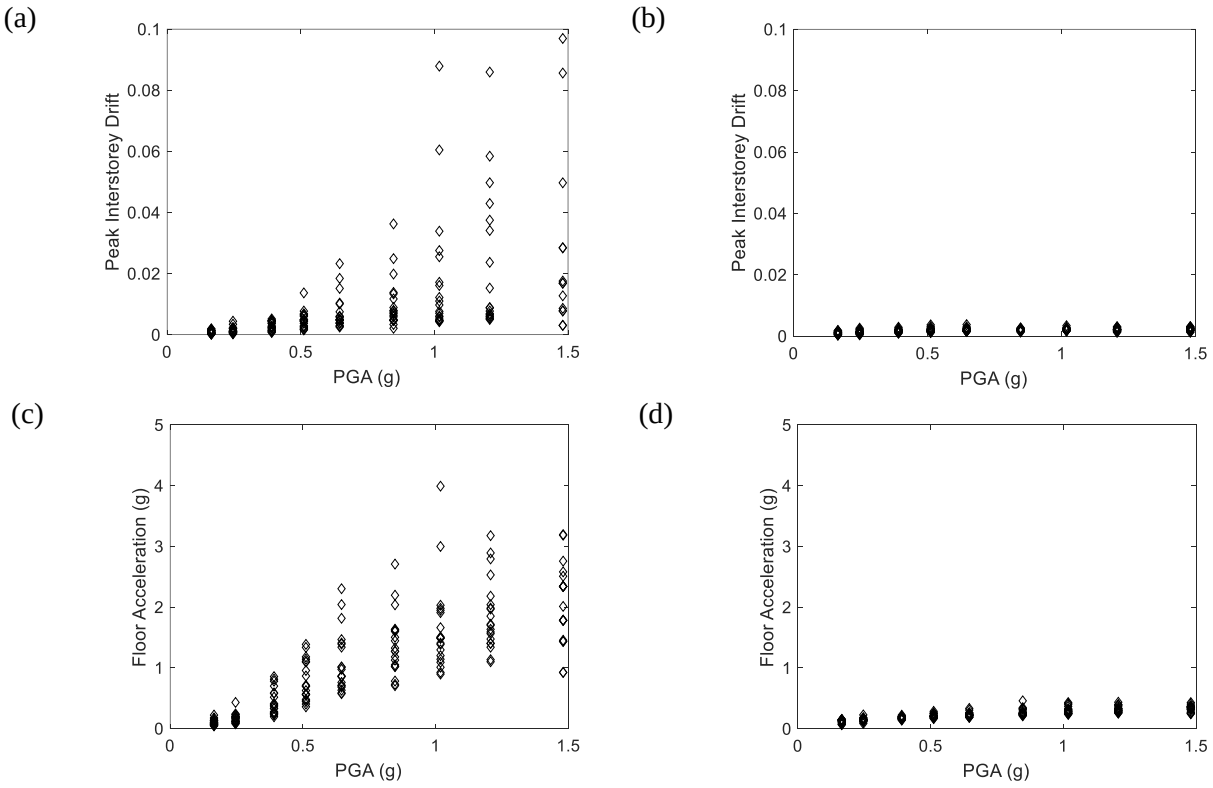

Fig. 5 – Comparison of NLTH dynamic analysis results for the fixed-base (left) and seismically isolated (right) RUAUMOKO light-frame wood building models.

At each PGA intensity for the fixed-base model (Fig. 5(a) and (c)), the median of the engineering demand parameter (EDP) can be determined. Considering the assumption that one third of the losses are due to acceleration sensitive components, two thirds are due to drift sensitive components, the damage ratio for acceleration, and drift-sensitive components as a function of the median

engineering demand parameter were determined with the results shown in Fig. 6. These can be considered as median EDP dependent loss functions or storey loss functions. Similar functions can be determined for other confidence intervals although only median results are presented here.

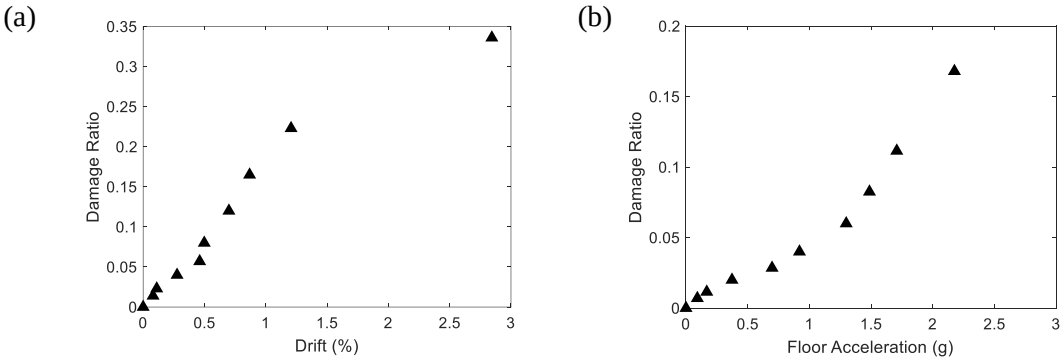

Fig. 6 – EDP dependent loss functions or storey loss functions, with loss expressed as the damage ratio for (a) roof acceleration and (b) interstorey drift.

3.5 Step 5: Analyse isolation model and use EDP functions to assess vulnerability

To determine the damage ratio for the isolated building, the median EDP at each intensity level were determined from Fig. 5(b) and (d). The EDP values are expected to be significantly lower with seismic isolation added. Then, using the EDP dependent loss functions determined in Step 2, the total median loss (damage ratio) was calculated as the sum of the median acceleration and median drift loss at each intensity level. The vulnerability functions of the original fixed-base building and of the seismically isolated model are compared in Fig. 7. The flat shape of the seismically isolated vulnerability function for intensities greater than ≈0.4 g is expected as the acceleration in the superstructure is limited by the low friction interface between the concrete diaphragm and the input ground motions. Therefore, particularly in large shaking events, the expected loss to an isolated building is significantly reduced compared to a fixed-base counterpart.

4 Comparison of Expected Annual Loss

EAL can be used here to compare the likely performance of fixed-base and seismically isolated light-frame wood buildings. EAL can be calculated by integrating the loss through the hazard curve through:

$$\text{EAL} = \int_{IM} E[Loss|im]|d\lambda(im)| \tag{3}$$

where E[Loss|im] is the expected direct monetary loss for a given intensity measure, im, and λ(im) is the annual frequency of exceeding an earthquake intensity such that dλ(im) is the derivative of the hazard curve at intensity im [24]. Fig. 7(a) shows E[Loss|im], which is represented by the damage ratio, as a function of im which, in turn, is represented by the PGA. Note that at small intensities, the vulnerability of the seismically isolated building is shown to increase slightly. This is likely due to additional acceleration from the second mode of vibration but has not yet been verified as a real physical phenomenon.

EAL expressed as mean damage factors (MDF), defined as the repair cost normalized by the building replacement cost, was calculated for the fixed-base and seismically isolated building models with the results shown in Table 4. The fixed-base and isolated building models were found to have an EAL of 0.146% and 0.115% of the building replacement cost respectively. This represents average annual savings of 31% for the isolated building compared to the fixed-base alternative. Additional savings

would be possible with the use of lower friction systems than the system with a coefficient of 0.1 considered in this analysis. In addition, thoughts must be given to the non-cost related factors of seismic isolation, such as loss of functionality of the building for repair work to be undertaken as well as the stress of organizing insurance pay outs for earthquake damage, which was a major issue after the 2011 Christchurch Earthquake [25].

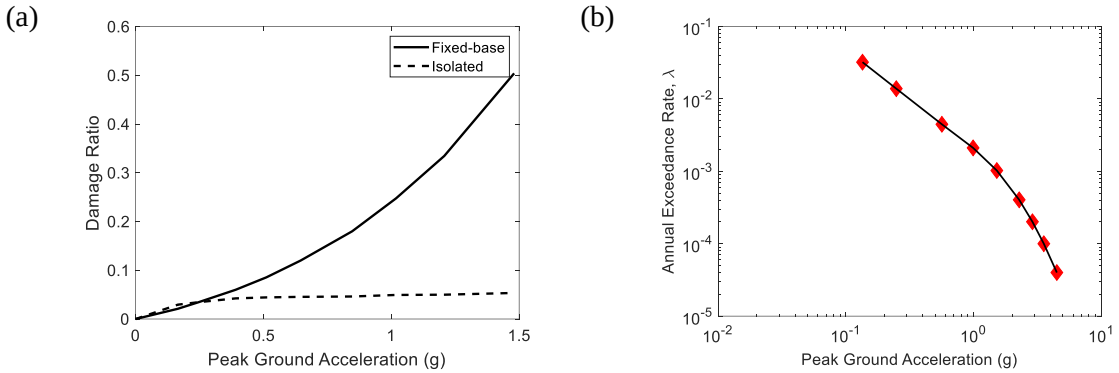

Fig. 7 –Comparison of (a) the fixed-base and seismically isolated light-frame wood building vulnerability functions and (b) the annual frequency of exceeding an earthquake intensity.

Table 4 – Calculation and comparison of the EAL for the fixed-base and seismically isolated models.

Intensity Measure (PGA)	**MAF, λ(im)**	**Occurrence Rates $\Delta\lambda_i$**	**MDF_{fixed}**	**$MDF_{isolated}$**	**EAL_{fixed}**	**$EAL_{isolated}$**
0.165	0.03219	0.0092	0.022345	0.029424	0.0205%	0.0270%
0.246	0.01386	0.0139	0.034805	0.034514	0.0483%	0.0478%
0.391	0.00446	0.0059	0.06035	0.04231	0.0355%	0.0249%
0.511	0.00211	0.0017	0.085451	0.044332	0.0147%	0.0076%
0.646	0.00103	0.0009	0.118535	0.045431	0.0101%	0.0039%
0.847	0.00040	0.0004	0.180359	0.046178	0.0074%	0.0019%
1.018	0.00020	0.0002	0.246561	0.049348	0.0037%	0.0008%
1.207	0.00010	0.0001	0.336437	0.049874	0.0027%	0.0004%
1.480	0.00004	0.0001	0.503442	0.053464	0.0035%	0.0004%
					0.146%	**0.115%**

5 Sensitivity Analyses

The EAL for the isolated building heavily depends on its vulnerability function. Initially, this vulnerability function (Fig. 7(a)) implies a steady state loss for PGA intensities greater than approximately 0.4 g. However, with increasing intensity, displacement demands would increase to a point where additional loss would be likely. Such loss would be attributed to damage from the system exceeding its displacement capacity and causing impact loading or rupture of flexible service connections to the building. In addition, there may be costs associated with re-centring after large residual displacements.

The isolated vulnerability function in Fig. 7(a) was modified such that after a selected intensity level, the curve follows the trajectory of the fixed-base building vulnerability function. An example is shown in Fig. 8(a), which shows the modified vulnerability function corresponding to loss increasing after IM level 6, which corresponds to a return period of 2% in 50 years (see Table 3).

The procedure was repeated for the remaining intensity levels and EAL was determined for each vulnerability function in the same procedure shown in Table 4. Fig. 8(b) is the culmination of these results and shows the EAL for each variant of the vulnerability function, versus the median isolator displacement at the given IM level where the vulnerability function begins matching that of the isolated building. Fig. 8(b) can be interpreted as showing the EAL for different isolator displacement capacities and thus becomes a useful metric for determining appropriate design values of displacement capacity.

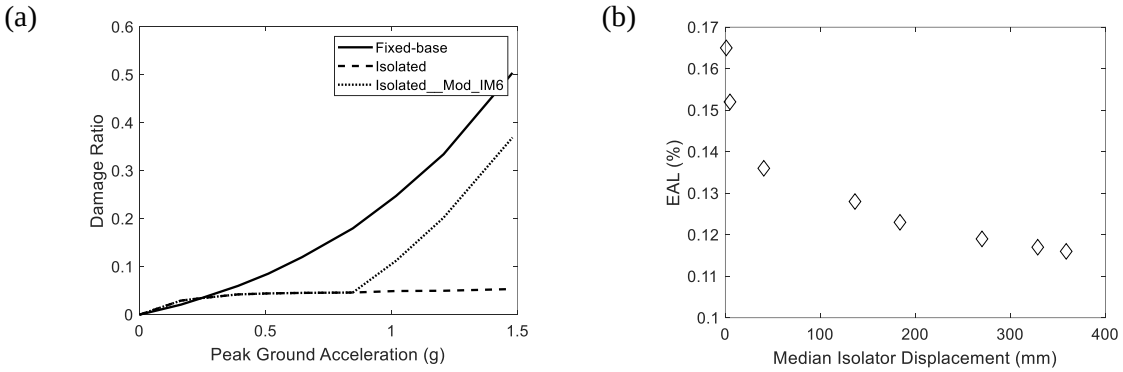

Fig. 8 – (a) Modification of the isolated vulnerability function and (b) the variation of EAL with the median peak isolator displacement.

6 Conclusion

Seismic isolation has not been widely considered for use in light-frame wood buildings in New Zealand, largely due to predicted cost and wind loading issues, which would cause buildings to move under high wind gusts. This paper presented a value case for using seismic isolation technology by demonstrating that significant cost savings can be obtained through comparison of EAL for fixed-base and seismically isolated buildings. For an isolation system with a friction coefficient of 0.1, the EAL to the building was 31% less compared to a fixed-base alternative. Such friction coefficient would be sufficient to resist wind loading in high wind regions of New Zealand without activating the seismic isolation system. Sensitivity analyses show that the EAL depends significantly on the vulnerability function of the seismically isolated building and an approach for estimating the required isolation system displacement was presented. Further research will build on the work done in Japan, the United States and New Zealand to propose a practical and cost-effective method for seismic isolation using a friction based approach with mass added to the floor diaphragm level to prevent movement under strong wind loads.

7 Acknowledgements

This project was (partially) supported by QuakeCoRE, a New Zealand Tertiary Education Commission-funded Centre. This is QuakeCoRE publication number 0534.

8 References

[1] A. Buchanan, D. Carradine, G. Beattie, H. Morris (2011): Performance of Houses during the Christchurch Earthquake of 22 February 2011. *Bulletin of the New Zealand Society for Earthquake Engineering*, **44** (4), 342–357.

[2] A. Filiatrault, B. Folz (2002): Performance-Based Seismic Design of Wood Framed Buildings. *Journal of Structural Engineering*, **128** (1), 39–47.

[3] Reserve Bank of New Zealand (2016): *Reserve Bank of New Zealand Bulletin - The Canterbury Rebuild Five Years on from the Christchurch Earthquake*.

[4] N. A. Horspool, A. B. King, S. L. Lin, S. R. Uma (2016): Damage and Losses to Residential Buildings during the Canterbury Earthquake Sequence. *2016 NZSEE Conference*, Christchurch, New Zealand.

[5] M. Iiba, M. Midorikawa, H. Yamanouchi, S. Yamaguchi, Y. Ohashi, M. Takayama (2000): Shaking Table Tests on Performance of Isolators for Houses Subjected to Three-Dimensional Earthquake Motions. *12th World Conference on Earthquake Engineering*, New Zealand.

[6] M. Iiba, M. Midorikawa, Y. Yamanouchi, M. Ikenaga, K. Machida (2001): Construction of a Base-Isolated House for Observation of Isolation Effects during Earthquake and Wind. *NIST SPECIAL PUBLICATION SP*, 203–212.

[7] T. Hanai, S. Nakata, S. Kiriyama, N. Fukuwa (2004): Comparison of Seismic Performance of Base-Isolated House with Various Devices. *13th World Conference on Earthquake Engineering*, 2004.

[8] S. J. Thurston (2006): *Base isolation of low rise light and medium weight buildings.* BRANZ Ltd.

[9] V. A. Zayas, S. S. Low (1997): Seismic Isolation of a Four-Storey Wood Building, *Earthquake Performance and Safety of Timber Structures*, 83–91.

[10] S. Swensen *et al.* (2014): Toward Damage Free Residential Houses through Unibody Light-Frame Construction with Seismic Isolation. *SEAOC 2014 83rd Annual Convention. Indian Wells*, USA.

[11] E. A. Jampole, G. Deierlein, E. Miranda, B. Fell, S. Swensen, C. Acevedo (2016): Full-Scale Dynamic Testing of a Sliding Seismically Isolated Unibody House, *Earthquake Spectra*, **32** (4), 2245–2270.

[12] E. A. Jampole, S. D. Swensen, B. Fell, E. Miranda, G. G. Deierlein (2014): Dynamic Testing of a Low-Cost Sliding Isolation System for Light-Frame Residential Structures. *Tenth US National Conference on Earthquake Engineering, Frontiers of Earthquake Engineering, Anchorage,* Alaska.

[13] R. Shelton (2013): *Engineering Basis of NZS 3604.*

[14] Standards New Zealand (2011): *NZS 3604:2011 - Timber-Framed Buildings*. Standards New Zealand.

[15] USGS (2016): *ShakeMap (software).*

[16] A. Carr (2018): *Ruaumoko 3D - Inelastic Dynamic Analysis Software*. Christchurch, New Zealand.

[17] S. J. Thurston (2003): *Full-sized house cyclic racking test.* BRANZ Ltd.

[18] A. Carr (2016): *Ruaumoko Manual - Volume 5: Appendices, Strength and Stiffness Degradation*. Carr Research Ltd.

[19] B. Folz, A. Filiatrault (2004): Seismic Analysis of Woodframe Structures. II: Model Implementation and Verification," *J. Struct. Eng.*, **130** (9), 1361–1370.

[20] W. Pang, E. Ziaei, A. Filiatrault (2012): A 3D Model for Collapse Analysis of Soft-Story Light-Frame Wood Buildings. *World Conference on Timber Engineering*, Auckland, New Zealand.

[21] T. Z. Yeow, A. Orumiyehei, T. J. Sullivan, G. A. MacRae, G. C. Clifton, K. J. Elwood (2018): Seismic Performance of Steel Friction Connections Considering Direct-Repair Costs. *Bulletin of Earthquake Engineering*, **16** (12), 5963–5993.

[22] K. Tarbali, B. A. Bradley (2015): Ground Motion Selection for Scenario Ruptures Using the Generalised Conditional Intensity Measure (GCIM) Method. *Earthquake Engineering & Structural Dynamics*, **44** (10), 1601–1621.

[23] B. A. Bradley, R. P. Dhakal, M. Cubrinovski, J. B. Mander, G. A. MacRae (2007): Improved Seismic Hazard Model with Application to Probabilistic Seismic Demand Analysis. *Earthquake Engineering and Structural Dynamics*, **36**, 2212–2225.

[24] T. J. Sullivan (2016): Use of Limit State Loss versus Intensity Models for Simplified Estimation of Expected Annual Loss. *Journal of Earthquake Engineering*, **20**, (6), 954–974.

[25] S. H. Potter, J. S. Becker, D. M. Johnston, K. P. Rossiter (2015): An Overview of the Impacts of the 2010-2011 Canterbury Earthquakes. *International Journal of Disaster Risk Reduction*, **14**, 6–14.

